

Article

Preparation of a New Active Component 1,10-B₁₀H₈(S(C₁₈H₃₇)₂)₂ for Potentiometric Membranes for the Determination of Terbinafine Hydrochloride

Eugeniy S. Turyshev ^{1,*}, Alexey V. Golubev ² , Alexander Yu. Bykov ², Konstantin Yu. Zhizhin ^{2,*} and Nikolay T. Kuznetsov ²

¹ Institute for African Studies of the Russian Academy of Sciences (IAS), st. Spiridonovka 30/1, Moscow 123001, Russia

² N.S. Kurnakov Institute of General and Inorganic Chemistry of the Russian Academy of Sciences, Leninskii pr.31, Moscow 119991, Russia

* Correspondence: tyrishev@gmail.com (E.S.T.); kyuzhizhin@igic.ras.ru (K.Y.Z.)

Abstract: This paper presents a methodology for the preparation of a new active component for ion-selective membranes, based on a di-substituted sulfonium derivative of the *closo*-decaborate anion at the apical vertices with the octadecylalkyl substituents 1,10-B₁₀H₈(S(C₁₈H₃₇)₂)₂. This approach is characterized by physicochemical methods of analysis (11B, 1H, 13C NMR spectroscopy, IR spectroscopy and elemental analysis). The compound obtained is used as an active component of a PVC membrane selective to terbinafine hydrochloride. The sensor developed is highly selective to the drug to be detected, has a linearity range of 4.0×10^{-8} – 1.0×10^{-2} and a detection limit of 1.0×10^{-8} , and can detect terbinafine hydrochloride in the pH range of 3 to 6.

Keywords: polymers; ion-selective membrane; boron clusters; sulfanyl derivative; terbinafine



Academic Editor: Michael A. Beckett

Received: 26 November 2024

Revised: 15 January 2025

Accepted: 23 January 2025

Published: 24 January 2025

Citation: Turyshev, E.S.; Golubev, A.V.; Bykov, A.Y.; Zhizhin, K.Y.; Kuznetsov, N.T. Preparation of a New Active Component 1,10-B₁₀H₈(S(C₁₈H₃₇)₂)₂ for Potentiometric Membranes for the Determination of Terbinafine Hydrochloride. *Inorganics* **2025**, *13*, 35. <https://doi.org/10.3390/inorganics13020035>

Copyright: © 2025 by the authors. Licensee MDPI, Basel, Switzerland. This article is an open access article distributed under the terms and conditions of the Creative Commons Attribution (CC BY) license (<https://creativecommons.org/licenses/by/4.0/>).

1. Introduction

The availability and purification of water resources are a basic priority for humanity in general and for the scientific community in particular. According to the UN [1], 2.2 billion people do not have access to clean drinking water, 3.5 billion people do not have access to safe sanitation and 80% of wastewater is returned to the ecosystem without treatment. The issue of water resources is particularly acute in Africa, in arid climate zones [2], where there is also steady and continuous population growth [3], as well as a significant requirement for water resources for the extraction of numerous minerals [4].

Anthropogenic nitrogen [5–7], which is contained in fertilizers, herbicides and fungicides, is an important factor in hydrosphere pollution, especially in water bodies located in the agricultural zone. Nitrogen-containing compounds play an important role in the modern world, but their content should be controlled.

Potentiometry is one of the best methods of control. Due to its rapidity, simplicity and low cost, the ionometric method can be implemented in field conditions, in treatment plants and in analytical laboratories [8]. There are, however, a limited set of ions that can be determined by potentiometry [9]. Recently, the search for new active components for selective membranes has been re-emphasized [10]. The combination of the potentiometric method of analysis with other methods, such as HPLC [11], allows the design of highly accurate analytical systems with wide customizability and high application potential. The

development of synthetic chemistry and materials science has made it possible to create complex macromolecular systems that are selective toward organic ions with a delocalized charge [12]. Such sensors are highly selective to a particular ion and enable analysis of systems consisting of similar molecules.

It has previously been shown that *closo*-decaborates with exopolyhedral functional substituents can be used in ion-selective membranes for the detection of various classes of organic compounds, such as local anesthetics, hormones and quaternary ammonium bases, including biodegradable compounds that can accumulate in aqueous media [13].

Terbinafine is an antifungal drug, first produced in 1984 [14] and tested in 1989 [15], which has shown promising results; its structure is shown in Figure 1. Included in the WHO's list of essential drugs, it belongs to the class of derivatives of allylamine [16]. Its principle of action is to disrupt the integrity of the cytoplasmic membrane of fungi and block the synthesis of membrane sterols [17]. In tablet or ointment form, it is used for the treatment of variegated shingles, fungal infections of the nails and ringworm, and for addressing itching and mycosis. Terbinafine is an effective fungicidal agent that causes minimal adverse reactions [18,19] and is effectively used for the treatment of both humans and animals [20]. Many studies are currently underway to expand the use of this drug [21,22].

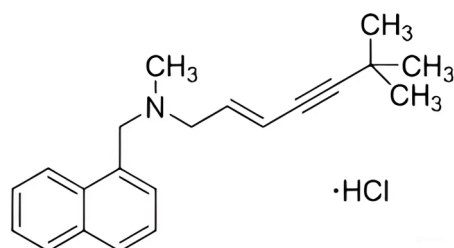


Figure 1. Chemical structure of terbinafine hydrochloride.

For the analytical determination of terbinafine, HPLC [23] with a detection limit of up to 1.0×10^{-8} M is mainly used. In the literature, a limit of quantification up to 2.7×10^{-7} M [24] is indicated. The measurement uncertainty in the determination of terbinafine by HPLC with UV detection was evaluated in [25]. Other methods used for the qualitative and quantitative analysis of terbinafine hydrochloride, in the form of tablets, creams, plasma and other biological samples, have included UV, LC/MS, UPLC, HPLC, GC/MS, HPTLC, GC, ion-pair electrophoresis, micellar chromatography and UFLC [26]. In 2013, for the first time, a potentiometric sensor based on tetraphenylborate was reported to have successfully determined terbinafine in pharmacological preparations [27]. Since then, the electrochemical analysis of terbinafine has been actively developed [28]. Potentiometric determination appears to be the most promising approach due to its rapidity, portability, simplicity, low cost of analysis and low limit of detection [29].

As can be seen from Table 1, the ion-pair complex of the terbinafine cation and tetraphenyl borate anion is the main active component for the potentiometric determination of terbinafine. It has previously been shown that lipophilic boron cluster anions have greater selectivity to organic cations [30]. Therefore, the question of the functionalization of boron cluster anions and the investigation of the electroanalytical properties of membranes with them in their composition remain relevant.

Table 1. Some potentiometric sensors for detecting terbinafine hydrochloride.

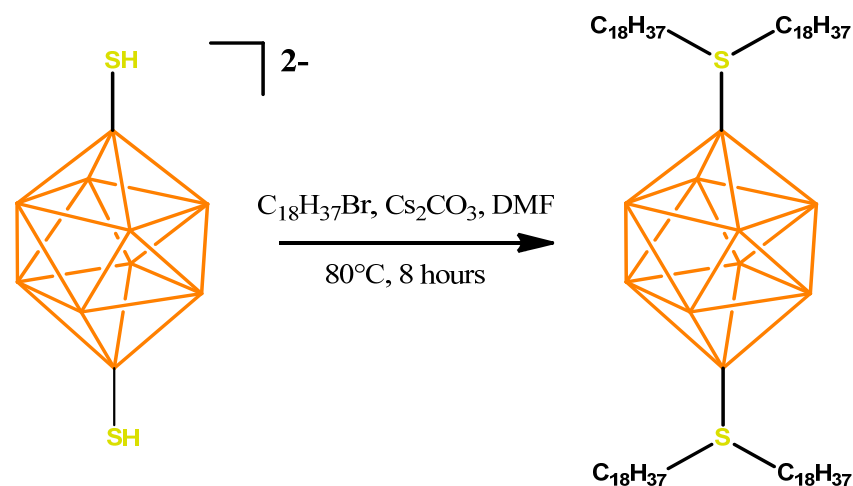
Active Membrane Ingredient	Linear Range, M	LOD, M	References
Terbinafine screen-printed microchip modified with MWCNTs	1.0×10^{-2} – 1.0×10^{-8}	5.0×10^{-9}	[28]
Ion-pair terbinafine and tetraphenyl borate functionalized CaO/ZnO	1.0×10^{-2} – 7.0×10^{-6}	6.5×10^{-6}	[27]
Sodium tetraphenylborate	1.0×10^{-2} – 1.0×10^{-6}	7.9×10^{-7}	[29]
Ion-pair terbinafine and tetraphenyl borate functionalized CaO/ZnO	1.0×10^{-2} – 5.0×10^{-9}	2.5×10^{-10}	[31]

This study describes the synthesis of a new *closo*-borate compound, 1,10- $B_{10}H_8(S(n-C_{18}H_{37}))_2$ —1,10-di-(bis-octodecylsulfonio)-*closo*-decaborate, and investigates its physico-chemical characteristics. Membranes selective to terbinafine ions are obtained on the basis of the new compound, and their potentiometric parameters and operational characteristics are studied.

2. Results

2.1. Synthesis of the Active Ingredient

The preparation of the disubstituted sulfonium derivative of the *closo*-decaborate anion with octadecylalkyl substituents 1,10- $B_{10}H_8(S(n-C_{18}H_{37}))_2$ can be carried out using a similar procedure to that used for the mono-substituted sulfonyl derivative $[2-B_{10}H_9SH]^{2-}$ [32]. Due to the presence of two functional groups, however, a longer reaction time is needed. The general scheme for the preparation is presented below (Figure 2).

**Figure 2.** Scheme for the synthesis of 1,10- $B_{10}H_8(S(n-C_{18}H_{37}))_2$.

The progress of the reaction can be monitored using ^{11}B NMR spectroscopy. In the ^{11}B NMR spectrum (Figure S2), all the signals relative to the parent compound $Cs_2[B_{10}H_8(SH)_2]$ [33] shifted to the weak field: from the apical vertices by 4.7 ppm, whereas from the equatorial ones by 0.6 ppm, and they are at 9.2 and -24.4 ppm, respectively. In addition, the shape of the signals changed significantly and a strong broadening of the signals was observed. The width of the signal at half its height was 586 Hz for the apical

vertices and 134 Hz for the equatorial vertices; for the anion $[1,10\text{-B}_{10}\text{H}_8(\text{SH})_2]^{2-}$, these values were 4.7 and 5.6 Hz, respectively.

According to the ^1H NMR spectroscopy data for the final product, several signals relating to the organic part of the target compound can be observed. The signal at 3.26 ppm refers to methylene groups bound to the sulfur atom; these groups were diastereotopic and were located at the prochiral S-center, resulting in the shape of this signal being a doublet of doublet triplets with the constants $J_1 = 91.5$ Hz, $J_2 = 12.8$ Hz and $J_3 = 7.2$ Hz, with the presence of a roof effect (Figure S1). The signals at 2.02, 1.54, 1.35 and 1.26 ppm can be attributed to the remaining methylene groups in the alkyl substituent, with the signal at 0.89 ppm relating to the C18 methyl group. In the ^{13}C NMR spectrum, a group of signals related to the octadecylalkyl substituent can also be observed. The signal at 43.67 ppm refers to the methylene group bonded to the sulfur atom.

2.2. Ion Sensor Development

The electrochemical response and potential measurement (E_m) of membranes are governed by three key mechanisms. At the core of these processes lies a sophisticated interaction: the membrane's ability to selectively transport ions across its interface with solutions, ionic mobility within its structure and the hydrophobic forces that develop between organic membrane elements and ions. These fundamental phenomena, involving transport dynamics and molecular forces, ultimately determine the electrode's selective capabilities and electrical characteristics, which have been mathematically described [34,35]:

$$E_m = \text{const} + (RT/z_X F) \ln(c_{aq}^X/c_m^X) = \text{const} + (RT/z_X F) [\ln c_{aq}^X + \ln(K_{ass}^{XY} c_m^Y/c_m^{XY})]$$

where c_{aq}^X is the concentration of the terbinafine cation (X) in the test solution; z_X is the charge of the terbinafine cation; c_m^X , c_m^Y and c_m^{XY} reveals the concentrations of the terbinafine cation (X), counter-anion (Y) and joint ion-pair complex (XY) in the membrane; K_{ass}^{XY} is the association constant of the ion-pair complex; F is the Faraday constant; R is the gas constant; and T is absolute temperature. This means that the lipophilicity of a primary ion (X) and a counter-ion (Y) and the association degree of their ion-pair complex in the membrane phase are the main factors affecting the electroanalytical characteristics of the sensor.

The selection of a suitable plasticizer (solvent mediator) is crucial for optimizing ionic sensor performance, as it plays a dual role in the membrane system. By determining the dielectric and mechanical characteristics of the polymeric membrane, while also facilitating the movement of membrane-forming components, the plasticizer serves as an essential element in the membrane composition that cannot be overlooked.

As was shown earlier, the best potentiometric parameters are shown by membranes with a low dielectric constant plasticizer according [12] to the Igen–Denison–Ramsey–Fuoss equation ($T = 293$ K) [36], so we have chosen aliphatic BBPA ($\epsilon_r = 5.3$).

The potentiometric curve characterizing the response of the sensor based on the PVC membrane containing $1,10\text{-B}_{10}\text{H}_8(\text{S}(n\text{-C}_{18}\text{H}_{37})_2)_2$ in BBPA to the terbinafine ion selected is shown in Figure 3. As can be seen, the sensor showed close to Nernstian slopes of 57.2 ± 0.2 mV/decade over a wide linear concentration range for all the tested solutions.

The terbinafine ion-selective membrane sensors were calibrated and the potentiometric selectivity coefficients were determined. The potentiometric response characteristics of the sensor were found to be dependent on the amount of terbinafine salt in the membrane composition (see Table 2).

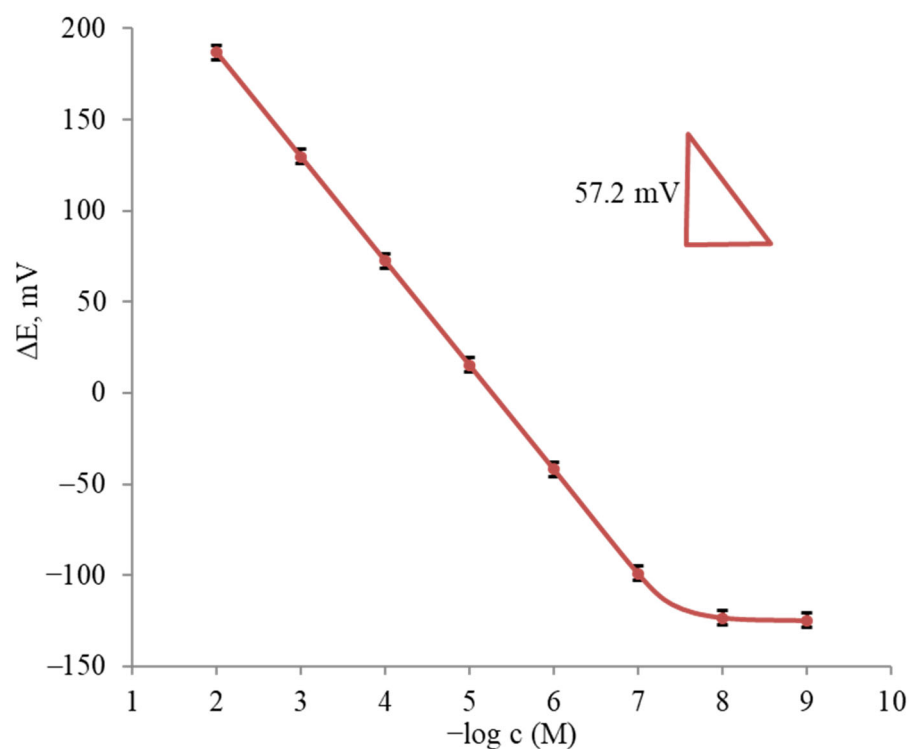


Figure 3. Average potentiometric curve for the determination of terbinafine hydrochloride ($n = 5$).

Table 2. Parameters of sensors containing different levels of active components.

№	Membrane Composition, % wt			Linear Range, M	Lower Detection Limit, M	Slope, mV/Decade
	1,10-B ₁₀ H ₈ (S(<i>n</i> -C ₁₈ H ₃₇) ₂) ₂	BBPA	PVC			
1	1.0	70.0	29.0	$\approx 10^{-8}$ – 10^{-2}	$\approx 5.0 \times 10^{-9}$	60 ± 2
2	1.2	69.8	29.0	$\approx 10^{-8}$ – 10^{-2}	$\approx 6.0 \times 10^{-9}$	59 ± 1
3	1.4	69.6	29.0	$\approx 2.0 \times 10^{-8}$ – 10^{-2}	$\approx 7.0 \times 10^{-9}$	58.2 ± 0.5
4	1.6	69.4	29.0	$\approx 3.0 \times 10^{-8}$ – 10^{-2}	$\approx 8.0 \times 10^{-9}$	57.7 ± 0.3
5	1.8	69.2	29.0	4.0×10^{-8} – 10^{-2}	1.0×10^{-8}	57.2 ± 0.2
6	2.0	69.0	29.0	8.0×10^{-8} – 10^{-2}	3.0×10^{-8}	55.9 ± 0.2
7	2.2	68.8	29.0	10^{-7} – 10^{-2}	5.0×10^{-8}	53.6 ± 0.2
8	2.4	68.6	29.0	3.0×10^{-7} – 10^{-2}	7.0×10^{-8}	52.3 ± 0.2

As follows from the results obtained, the sensor based on membrane no. 5 had the best content. This sensor showed a Nernstian response in the concentration range of 4.0×10^{-8} – 10^{-2} M and a lower detection limit (LOD) of 1.0×10^{-8} M. In addition, the sensor showed stability, good reproducibility and a fast response. The interference of some common cations in some sensors' response was studied using the mixed solution method. Potentiometric measurements were carried out using test solutions containing the constant concentration of an interfering ion (0.01 M). The calculated selectivity coefficient values are shown in Table 3. These values clearly indicate that the terbinafine sensor was fairly selective toward the terbinafine cations for the different ions tested.

Table 3. Selectivity coefficients.

Interfering Cation	$\lg K^{\text{pot}}_{\text{Terbinafine/Cation}}$		
	MPM	Middle	SSM
Li ⁺	−3.41	−4.12	−4.83
Na ⁺	−3.37	−3.85	−4.33
K ⁺	−3.80	−3.91	−4.02
Rb ⁺	−3.16	−3.96	−4.76
Cs ⁺	−3.63	−4.18	−4.73
Ca ²⁺	−4.03	−4.64	−5.25
Sr ²⁺	−4.17	−4.73	−5.29
Ba ²⁺	−4.45	−5.02	−5.59
NH ₄ ⁺	−2.52	−3.29	−4.06
Glycine	−3.32	−3.72	−4.12
Valine	−3.42	−3.68	−3.94
β-Alanine	−3.25	−3.52	−3.79
L, D-Tyrosine	−3.01	−3.21	−3.41
Tetrabutylammonium ⁺ (TBA ⁺)	−2.32	−3.01	−3.70
Glucose	−4.56	−4.75	−4.94
Fructose	−4.66	−4.78	−4.90
Sucrose	−4.63	−4.82	−5.01

The active component 1,10-B₁₀H₈(S(*n*-C₁₈H₃₇)₂)₂ is a neutral carrier, but the membranes obtained showed no response to inorganic anions. This may have been because the boron backbone [B₁₀H₈]^{2−} has a constant negative charge. Due to their structure, the lipophilic S⁺(*n*-C₁₈H₃₇)₂ groups were embedded in the polymer matrix of the PVC and the charge on the sulfur atom was partially shielded. It can be observed from Table 3 that more lipophilic cations (TBA⁺) had a greater interfering effect.

Following established IUPAC guidelines [37], we conducted comprehensive testing of the sensor capabilities. Two distinct approaches—the matched potential method (MPM) and separate solution method (SSM)—were employed to measure the selectivity coefficients potentiometrically, which effectively addressed the challenges posed by interfering ions' non-Nernstian responses [38].

The dynamic response time is the time required for the electrode to achieve values within ±1 mV of the final equilibrium potential after successive immersions in the sample solutions [39]. Its calculation involved varying and recording the terbinafine concentration in a series of solutions from 1.0 × 10^{−2} to 1.0 × 10^{−8} M. The sensors were able to quickly reach their equilibrium response in the whole concentration range. The time of this for the PVC membrane electrode was about 20 s in the concentrated solutions. The sensor displayed good storage characteristics, and it was used over about six months (100 measurements) without significant deviation in the slope and LOD. The potential in a certain control solution remained virtually the same (±0.5 mV) during the whole lifetime of the sensor.

To examine the effect of the pH on the electrode responses, the potential was measured at specific concentrations of the terbinafine solution (1.0 × 10^{−4} M) for pH values ranging from 1.0 to 9.0 (concentrated NaOH or HCl solutions were used for the pH adjustment) for each of the PVC membrane electrodes, Figure 4. The results have shown that the potential

remained constant despite the pH changes within the range of three to six, which indicates the applicability of this electrode in the specified pH range. Some quite noteworthy fluctuations in the behavior of the potential as the pH changed were observed below and above the aforementioned pH limits. Specifically, fluctuations above a pH value of six might be justified by removing the positive charge on the drug molecule. Fluctuations below a pH value of three were caused by the removal of the membrane ingredients or the analyte in the solution.

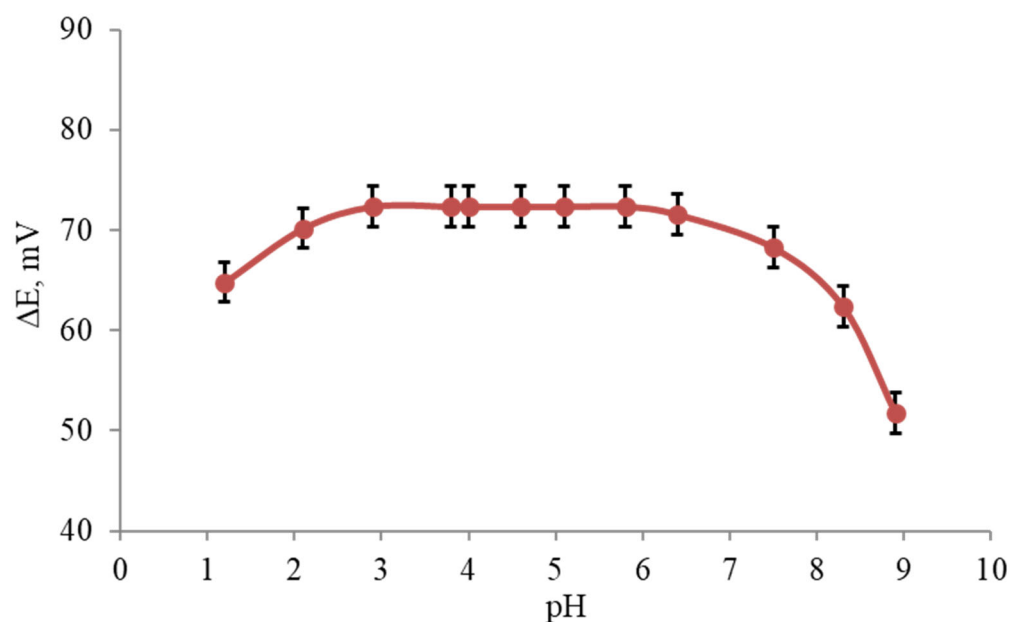


Figure 4. Average pH effect of the test solution (1.0×10^{-4} M) on the potential response of terbinafine hydrochloride ($n = 5$).

3. Materials and Methods

3.1. Analyses and Reagents

The elemental analysis of carbon, hydrogen and sulfur was performed using a Carlo Erba CHNS-3 FA 1108 automated elemental analyzer (Emmendingen, Germany).

The ^1H , ^{11}B and ^{13}C NMR spectra of the samples dissolved in CDCl_3 were recorded on a QOne AS400 (Wuhan, China) spectrometer (at the Shared Facility Center for Physical Research Methods of the Kurnakov Institute of General and Inorganic Chemistry of the Russian Academy of Sciences), operating at a frequency of 399.88, 128.29 and 100.55 MHz, respectively, using an internal deuterium lock. Tetramethylsilane and boron trifluoride etherate were used as external references. The NMR spectra of compound **1** are shown in Figures S1–S4.

The IR spectra of the complexes were recorded on a Lumex Infracum FT-02 Fourier-transform spectrophotometer in the range of $4000\text{--}400\text{ cm}^{-1}$, at a resolution of 1 cm^{-1} . The samples were prepared as pressed tablets with KBr. The IR spectra of compound **1** are shown in Figure S5.

All the reagents and chemicals used throughout this work were of analytical reagent grade and the solutions were prepared with redistilled water. High-molecular-weight poly(vinyl chloride) (PVC) with an average $M_w \sim 62,000$, tetrahydrofuran (THF) $\geq 99.0\%$, dichloromethane (CH_2Cl_2) $\geq 99.8\%$, petroleum ether, bis(1-butylpentyl)adipate (BBPA) $\geq 98.0\%$, terbinafine hydrochloride $\geq 98\%$, 1-bromooctadecane ($\text{C}_{18}\text{H}_{37}\text{Br}$) $\geq 97.0\%$, cesium carbonate (CsCO_3) 99% and dimethylformamide (DMF) 99.8% were purchased from Merck KGaA and used without prior purification. Cesium 1,10-bis(sulfanyl)-*closo*-decaborate Cs [1,10- $\text{B}_{10}\text{H}_9(\text{SH})_2$] was synthesized and identified in the Chemistry of Light

Elements and Clusters Laboratory of the N.S. Kurnakov Institute of General and Inorganic Chemistry of RAS [33]. Stock standard solutions of terbinafine hydrochloride (0.1 M and 1000 $\mu\text{g mL}^{-1}$) were prepared by dissolving precise amounts of each compound in water, 0.1 M HCl–NaOH or acetate buffer solutions. Working standard solutions were prepared daily from stock solutions by serial dilution. All the stock solutions were refrigerated between uses. The commercial pharmaceuticals analyzed in this study were purchased at a local pharmacy. The test samples of terbinafine hydrochloride were prepared by diluting 100–500 μL of each injectable solution up to 100.0 mL with 0.1 M acetate buffer solution (pH 4.67). These model solutions were subjected to the multiple standard additions procedure for determination.

3.2. Synthesis of 1,10-B₁₀H₈(S(*n*-C₁₈H₃₇)₂)₂

The salt Cs₂[1,10-B₁₀H₈(SH)₂] (200 mg, 0.45 mmol) was dissolved in 10 mL DMF in a 50 mL round-bottom flask, after which 1-bromooctadecane (625 mg, 1.87 mmol) and cesium carbonate (307.9 mg, 0.95 mmol) were added. The reaction solution was heated at 80 °C for 8 h, with constant stirring, in an argon atmosphere. The mixture was then evaporated using a rotary evaporator and dried from residual DMF in a deep vacuum using a rotary vane pump. Next, 10 mL of dichloromethane was added to the resulting residue, followed by treatment in an ultrasonic bath for 10 min. Then, the suspended mixture was centrifuged from the residue of cesium carbonate, so that cesium bromide was formed. The organic fraction was collected and evaporated again using a rotary evaporator. The residual octadecyl bromide was removed by flash chromatography on silica gel. For this, the substance was homogenized in 50 mL of petroleum ether and 1 g of SiO₂ silica gel in a 100 mL flask. It was then carefully evaporated and the resulting powder was placed on a chromatographic column pre-filled with pure silica gel. Petroleum ether was used as a washing eluent. The substance was collected from silica gel using a CH₂Cl₂/petroleum ether 1:1 mixture. The second organic fraction was collected and evaporated using a rotary evaporator and dried in a deep vacuum. 1,10-B₁₀H₈(S(*n*-C₁₈H₃₇)₂)₂ (440.7 mg, 0.37 mmol) was obtained (yield 82%).

Calcd. for C₇₂H₁₅₆B₁₀S₂, %: C, 72.41; H, 13.17; S, 5.37. Found, %: C, 72.29; H, 13.08; S, 5.32.

¹¹B{¹H} NMR (CDCl₃, ppm): 9.2 (s, 2B, B1, B10), –24.4 (d, 8B, B2–B9).

¹H NMR (CDCl₃, ppm): 3.26 (dm, 8H, SCH₂), 2.02 (m, 8H, SCH₂CH₂), 1.54 (m, 8H, C3H₂), 1.26 (m, 112H, C4H₂–C17H₂), 0.89 (t, 12H, CH₃), 1.80–0.20 (m, 8H, B₁₀H₈).

¹³C NMR (CDCl₃, ppm): 43.67 (SCH₂), 32.07 (SCH₂CH₂), 29.85, 29.80, 29.75, 29.66, 29.54, 29.51, 29.15, 28.82, 26.34 (C3–C16), 22.83 (CH₂CH₃), 14.26 (CH₃).

IR (KBr, cm^{−1}): 2955, 2918, 2850, 2505, 1467, 1417, 1378, 1314, 1263, 1247, 1227, 1177, 1129, 1097, 1067, 990, 963, 923, 890, 874, 852, 823, 795, 755, 721.

3.3. Manufacturing Membranes

Various membrane formulations, detailed in Table 2, were explored to develop a sensor with optimal potentiometric performance. The preparation process began with dissolving the constituent materials in tetrahydrofuran (THF) that had been previously distilled. The mixture underwent a thorough blending process, followed by a 5 min ultrasonic degassing treatment. Subsequently, the prepared solution was poured into a circular glass fixture (internal diameter: 28 mm) positioned on a flat glass platform. The membrane formation concluded when the THF completely evaporated after approximately three days at ambient temperature, yielding a clear polymer film.

To guarantee consistent membrane performance, precise control over the solvent evaporation and membrane thickness was maintained, while the components were meticulously

blended. The resulting membrane, with a thickness of 3 mm, was carefully developed. After the primary membrane was successfully detached from its glass surface, circular sections measuring approximately 6 mm in diameter were precisely excised. The final step involved placing these membrane disks into a specialized electrode housing (IS 561 model from Philips, Eindhoven, Netherlands), which was subsequently filled with terbinafine hydrochloride solution at a concentration of 1.0 mM.

Prior to the measurements, membrane equilibration was achieved by immersing the sensors in terbinafine hydrochloride solution (1.0 mM) for 24 h. For optimal performance in the trace analysis, conditioning the PVC membrane in a solution matching the sample composition enhanced the response times. The sensors required thorough cleaning with deionized distilled water after each measurement, followed by gentle drying using tissue paper. During storage periods, the electrodes were maintained in a dark, sealed container under dry conditions to ensure longevity and accuracy.

3.4. Potentiometric Measurements

The experimental setup involved a pH/ion analyzer from Radelkis (model OP-300, Budapest, Hungary) for conducting all the potentiometric tests. These measurements were performed under constant stirring conditions at ambient temperature ($25\text{ }^{\circ}\text{C} \pm 2\text{ }^{\circ}\text{C}$). A schematic diagram of the electrochemical cell follows:

Ag/AgCl	1.0 mM terbinafine hydrochloride	PVC membrane	Sample solution	AgCl _{satd} , 3M KCl	AgCl/Ag
---------	----------------------------------	--------------	-----------------	-------------------------------	---------

The measuring system incorporated a potentiometric sensor built using a Philips IS-561 electrode housing, coupled with an OP-0820 Radelkis (Budapest, Hungary) silver chloride reference electrode. For the pH determinations, the researchers employed a combination electrode (Radelkis OP-0808R) (Budapest, Hungary) alongside standardized Mettler Toledo buffer solutions for calibration.

4. Conclusions

In summary, a new compound, 1,10-di-(bis-octodecylsulfonio)-*closo*-decaborate—1,10-B₁₀H₈(S(C₁₈H₃₇)₂)₂ from Cs[1,10-B₁₀H₉(SH)₂], was obtained and a selective potentiometric sensor for terbinafine hydrochloride was obtained based on the new boron cluster compound. The sensor demonstrated advanced performance, with a fast response time (20 s), a lower detection limit of 1.0×10^{-8} M for the PVC membrane electrode and potential responses across the range of 4.0×10^{-8} – 1.0×10^{-2} M sloped 57.2 ± 0.2 . The obtained sensor was stable in the range of pH 3–6, which coincides with most of the aqueous media under study.

This study of potentiometric sensors with *closo*-borate compounds has contributed to the search for an effective express method for the determination of difficult organic compounds, particularly nitrogen-containing compounds, in water resources. This paper aimed to demonstrate the synthesis of a novel boron cluster compound and its potential applications in potentiometric sensors. The new active component has better characteristics than sodium tetraphenylborate, which provides great opportunities for modification of the sensor obtained; for example, introduction of an additional component into the membrane composition or reduction of the sensor design. The question of the influence of different classes of plasticizers with different dielectric constants on the membrane properties and the selectivity of the obtained sensor to substances similar in chemical structure to terbinafine also remains open. Advanced analytical studies and the development of a valid method

for the determination of terbinafine using the resulting sensor will be able to answer these questions.

Supplementary Materials: The following supporting information can be downloaded at <https://www.mdpi.com/article/10.3390/inorganics13020035/s1>, Figure S1: $^{11}\text{B}\{^1\text{H}\}$ NMR spectra of $1,10\text{-B}_{10}\text{H}_8(\text{S}(n\text{-C}_{18}\text{H}_{37})_2)_2$; Figure S2: ^{11}B NMR spectra of $1,10\text{-B}_{10}\text{H}_8(\text{S}(n\text{-C}_{18}\text{H}_{37})_2)_2$; Figure S3: ^1H NMR spectra of $1,10\text{-B}_{10}\text{H}_8(\text{S}(n\text{-C}_{18}\text{H}_{37})_2)_2$; Figure S4: ^{13}C NMR spectra of $1,10\text{-B}_{10}\text{H}_8(\text{S}(n\text{-C}_{18}\text{H}_{37})_2)_2$; Figure S5: IR spectra of $1,10\text{-B}_{10}\text{H}_8(\text{S}(n\text{-C}_{18}\text{H}_{37})_2)_2$.

Author Contributions: Conceptualization, E.S.T. and K.Y.Z.; methodology, E.S.T. and A.V.G.; software, A.Y.B.; validation, A.Y.B.; formal analysis, A.V.G.; investigation, E.S.T.; resources, N.T.K.; data curation, K.Y.Z.; writing—original draft preparation, E.S.T. and A.V.G.; writing—review and editing, K.Y.Z.; visualization, A.Y.B.; supervision, N.T.K.; project administration, N.T.K.; funding acquisition, K.Y.Z. All authors have read and agreed to the published version of the manuscript.

Funding: This article was prepared within the project “The ‘Clean Water’ project as the most important component of cooperation between the Russian Federation and the countries of the Global South: socio-economic and technological dimensions” supported by a grant from the Ministry of Science and Higher Education of the Russian Federation program for research projects in priority areas of scientific and technological development (Agreement № 075-15-2024-546).

Institutional Review Board Statement: Not applicable.

Data Availability Statement: Data are contained within the article.

Acknowledgments: This research was performed using the equipment of the JRC PMR IGIC RAS.

Conflicts of Interest: The authors declare no conflicts of interest. The funders had no role in the design of the study; in the collection, analyses, or interpretation of data; in the writing of the manuscript; or in the decision to publish the results.

References

1. Available online: <https://www.un.org/ru/global-issues/water> (accessed on 23 January 2025).
2. Agnew, C.; Anderson, E. *Water Resources in the Arid Realm*; Routledge: London, UK, 2024; ISBN 9781003463917.
3. Abramova, I.O. The Population of Africa under the Conditions of Transformation of the World Order. *Her. Russ. Acad. Sci.* **2022**, *92*, S1306–S1315. [[CrossRef](#)]
4. Abramova, I.O.; Sharova, A.Y. Geostrategic Risks in the Transition to Green Energies (Using the Example of Africa). *Geol. Ore Depos.* **2023**, *65*, 449–462. [[CrossRef](#)]
5. Yan, X.; Xia, Y.; Ti, C.; Shan, J.; Wu, Y.; Yan, X. Thirty Years of Experience in Water Pollution Control in Taihu Lake: A Review. *Sci. Total Environ.* **2024**, *914*, 169821. [[CrossRef](#)] [[PubMed](#)]
6. Qin, B.; Zhang, Y.; Zhu, G.; Gao, G. Eutrophication Control of Large Shallow Lakes in China. *Sci. Total Environ.* **2023**, *881*, 163494. [[CrossRef](#)]
7. Yu, S.; Du, X.; Lei, Q.; Wang, X.; Wu, S.; Liu, H. Long-Term Variations of Water Quality and Nutrient Load Inputs in a Large Shallow Lake of Yellow River Basin: Implications for Lake Water Quality Improvements. *Sci. Total Environ.* **2023**, *900*, 165776. [[CrossRef](#)]
8. Zdrachek, E.; Bakker, E. Potentiometric Sensing. *Anal. Chem.* **2021**, *93*, 72–102. [[CrossRef](#)]
9. Cuartero, M.; Colozza, N.; Fernández-Pérez, B.M.; Crespo, G.A. Why Ammonium Detection Is Particularly Challenging but Insightful with Ionophore-Based Potentiometric Sensors—An Overview of the Progress in the Last 20 Years. *Analyst* **2020**, *145*, 3188–3210. [[CrossRef](#)]
10. Ding, J.; Qin, W. Recent Advances in Potentiometric Biosensors. *TrAC Trends Anal. Chem.* **2020**, *124*, 115803. [[CrossRef](#)]
11. Gil, R.L.; Amorim, C.G.; Montenegro, M.C.B.S.M.; Araújo, A.N. HPLC-Potentiometric Method for Determination of Biogenic Amines in Alcoholic Beverages: A Reliable Approach for Food Quality Control. *Food Chem.* **2022**, *372*, 131288. [[CrossRef](#)]
12. Turyshev, E.S.; Kopytin, A.V.; Zhizhin, K.Y.; Kubasov, A.S.; Shpigun, L.K.; Kuznetsov, N.T. Potentiometric Quantitation of General Local Anesthetics with a New Highly Sensitive Membrane Sensor. *Talanta* **2022**, *241*, 123239. [[CrossRef](#)]
13. Turyshev, E.S.; Kubasov, A.S.; Golubev, A.V.; Zhizhin, K.Y.; Kuznetsov, N.T. Potentiometric Method for Determining Biologically Non-Degradable Antimicrobial Substances. *Russ. J. Inorg. Chem.* **2023**, *68*, 1841–1847. [[CrossRef](#)]

14. Stuetz, A.; Petranyi, G. Synthesis and Antifungal Activity of (E)-N-(6,6-Dimethyl-2-Hepten-4-Ynyl)-N-Methyl-1-Naphthalenemethanamine (SF 86-327) and Related Allylamine Derivatives with Enhanced Oral Activity. *J. Med. Chem.* **1984**, *27*, 1539–1543. [[CrossRef](#)] [[PubMed](#)]
15. Goodfield, M.J.D.; Rowell, N.R.; Forster, R.A.; Evans, E.G.V.; Raven, A. Treatment of Dermatophyte Infection of the Finger- and Toe-Nails with Terbinafine (SF 86-327, Lamisil), an Orally Active Fungicidal Agent. *Br. J. Dermatol.* **1989**, *121*, 753–757. [[CrossRef](#)]
16. Petranyi, G.; Ryder, N.S.; Stütz, A. Allylamine Derivatives: New Class of Synthetic Antifungal Agents Inhibiting Fungal Squalene Epoxidase. *Science (1979)* **1984**, *224*, 1239–1241. [[CrossRef](#)]
17. Ryder, N.S. Specific Inhibition of Fungal Sterol Biosynthesis by SF 86-327, a New Allylamine Antimycotic Agent. *Antimicrob. Agents Chemother.* **1985**, *27*, 252–256. [[CrossRef](#)]
18. Joly-Tonetti, N.; Legouffe, R.; Tomezyk, A.; Gumez, C.; Gaudin, M.; Bonnel, D.; Schaller, M. Penetration Profile of Terbinafine Compared to Amorolfine in Mycotic Human Toenails Quantified by Matrix-Assisted Laser Desorption Ionization–Fourier Transform Ion Cyclotron Resonance Imaging. *Infect. Dis. Ther.* **2024**, *13*, 1281–1290. [[CrossRef](#)]
19. Nakamura, T.; Yoshinouchi, T.; Okumura, M.; Yokoyama, T.; Mori, D.; Nakata, H.; Yasunaga, J.; Tanaka, Y. Antifungal Potency of Terbinafine as a Therapeutic Agent against *Exophiala Dermatitidis* in Vitro. *bioRxiv* **2024**. [[CrossRef](#)]
20. Viana, P.G.; Figueiredo, A.B.F.; Gremião, I.D.F.; de Miranda, L.H.M.; da Silva Antonio, I.M.; Boechat, J.S.; de Sá Machado, A.C.; de Oliveira, M.M.E.; Pereira, S.A. Successful Treatment of Canine Sporotrichosis with Terbinafine: Case Reports and Literature Review. *Mycopathologia* **2018**, *183*, 471–478. [[CrossRef](#)]
21. Pinto, Â.V.; Oliveira, J.C.; Costa de Medeiros, C.A.; Silva, S.L.; Pereira, F.O. Potentiation of Antifungal Activity of Terbinafine by Dihydrojasnone and Terpinolene against Dermatophytes. *Letts. Appl. Microbiol.* **2021**, *72*, 292–298. [[CrossRef](#)]
22. Li, M.; Chen, X.; Su, X.; Gao, W. The Preparation and Evaluation of a Hydrochloride Hydrogel Patch with an Iontophoresis-Assisted Release of Terbinafine for Transdermal Delivery. *Gels* **2024**, *10*, 456. [[CrossRef](#)]
23. Cox, S.; Hayes, J.; Hamill, M.; Martin, A.; Pistole, N.; Yarbrough, J.; Souza, M. Determining Terbinafine in Plasma and Saline Using HPLC. *J. Liq. Chromatogr. Relat. Technol.* **2015**, *38*, 607–612. [[CrossRef](#)]
24. Matysová, L.; Solich, P.; Marek, P.; Havlíková, L.; Nováková, L.; Šícha, J. Separation and Determination of Terbinafine and Its Four Impurities of Similar Structure Using Simple RP-HPLC Method. *Talanta* **2006**, *68*, 713–720. [[CrossRef](#)] [[PubMed](#)]
25. Separovic, L.; Lourenço, F.R. Measurement Uncertainty Evaluation of an Analytical Procedure for Determination of Terbinafine Hydrochloride in Creams by HPLC and Optimization Strategies Using Analytical Quality by Design. *Microchem. J.* **2022**, *178*, 107386. [[CrossRef](#)]
26. Gund, A.; Datar, P.A.; Kunjir, V.V. Analytical method development and validation of an allylamine antifungal drug, Terbinafine hydrochloride: A review. *Int. J. Nov. Res. Dev.* **2024**, *9*, a788–a815.
27. Faridbod, F.; Ganjali, M.R.; Norouzi, P. Potentiometric PVC Membrane Sensor for the Determination of Terbinafine. *Int. J. Electrochem. Sci.* **2013**, *8*, 6107–6117. [[CrossRef](#)]
28. El-Beshlawy, M.; Arida, H. Modified Screen-Printed Microchip for Potentiometric Detection of Terbinafine Drugs. *J. Chem.* **2022**, *2022*, 1–8. [[CrossRef](#)]
29. El-Rahman, M.K.A.; Sayed, R.A.; El-Masry, M.S.; Hassan, W.S.; Shalaby, A. Development of Potentiometric Method for In Situ Testing of Terbinafine HCl Dissolution Behavior Using Liquid Inner Contact Ion-Selective Electrode Membrane. *J. Electrochem. Soc.* **2018**, *165*, B143–B149. [[CrossRef](#)]
30. Kubasov, A.S.; Turishev, E.S.; Kopytin, A.V.; Shpigun, L.K.; Zhizhin, K.Y.; Kuznetsov, N.T. Sulfonium Closo-Hydridodecaborate Anions as Active Components of a Potentiometric Membrane Sensor for Lidocaine Hydrochloride. *Inorganica Chim. Acta* **2021**, *514*, 119992. [[CrossRef](#)]
31. Alterary, S.S.; Mostafa, G.A.E.; El-Tohamy, M.F.; Elhadi, A.M.; AlRabiah, H. A Novel Potentiometric Coated Wire Sensor Based on Functionalized Polymeric CaO/ZnO Nanocomposite Synthesized by *Lavandula Spica* Mediated Extract for Terbinafine Determination. *ChemistrySelect* **2024**, *9*, e202401217. [[CrossRef](#)]
32. Kubasov, A.S.; Turishev, E.S.; Polyakova, I.N.; Matveev, E.Y.; Zhizhin, K.Y.; Kuznetsov, N.T. The Method for Synthesis of 2-Sulfanyl Closo-Decaborate Anion and Its S-Alkyl and S-Acyl Derivatives. *J. Organomet. Chem.* **2017**, *828*, 106–115. [[CrossRef](#)]
33. Golubev, A.V.; Baltovskaya, D.V.; Kubasov, A.S.; Bykov, A.Y.; Zhizhin, K.Y.; Kuznetsov, N.T. Synthesis of 1,10-Disulfanyl-Closo-Decaborate Anion and Its Disulfonium Tetraacetylamide Derivative. *Russ. J. Inorg. Chem.* **2024**, 1–10. [[CrossRef](#)]
34. Freiser, H. (Ed.) *Ion-Selective Electrodes in Analytical Chemistry*; Springer: Boston, MA, USA, 1978; ISBN 978-1-4684-2594-9.
35. Bobacka, J.; Ivaska, A.; Lewenstam, A. Potentiometric Ion Sensors. *Chem. Rev.* **2008**, *108*, 329–351. [[CrossRef](#)]
36. Gordon, J. *Organic Chemistry of Electrolytes Solutions*; Mir: Moscow, Russia, 1979.
37. Buck, R.P.; Lindner, E. Recommendations for Nomenclature of Ionselective Electrodes (IUPAC Recommendations 1994). *Pure Appl. Chem.* **1994**, *66*, 2527–2536. [[CrossRef](#)]

38. Gadzekpo, V.P.Y.; Christian, G.D. Determination of Selectivity Coefficients of Ion-Selective Electrodes by a Matched-Potential Method. *Anal. Chim. Acta* **1984**, *164*, 279–282. [[CrossRef](#)]
39. Morf, W.E.; Lindner, E.; Simon, W. Theoretical Treatment of the Dynamic Response of Ion-Selective Membrane Electrodes. *Anal. Chem.* **1975**, *47*, 1596–1601. [[CrossRef](#)]

Disclaimer/Publisher’s Note: The statements, opinions and data contained in all publications are solely those of the individual author(s) and contributor(s) and not of MDPI and/or the editor(s). MDPI and/or the editor(s) disclaim responsibility for any injury to people or property resulting from any ideas, methods, instructions or products referred to in the content.